Journal of Materials Chemistry

Cite this: J. Mater. Chem., 2012, 22, 21720

www.rsc.org/materials

PAPER

# New sulfur-containing host materials for blue phosphorescent organic light-emitting diodes†

Jong-Kwan Bin,[a] JoongHwan Yang[b] and Jong-In Hong*[a]

*Received 27th June 2012, Accepted 3rd September 2012*
**DOI: 10.1039/c2jm34165d**

Two novel host materials based on carbazole derivatives were synthesized with benzo[*b*]thiophene (B2tCz) or dibenzothiophene (DB2tCz) for use in evaporation-processed blue phosphorescent organic light-emitting diodes. Both host materials exhibited high glass transition temperatures ($T_g = 179$ °C for B2tCz and $T_g = 185$ °C for DB2tCz) and triplet energy levels ($E_T = 2.84$ eV for B2tCz and $E_T = 2.93$ eV for DB2tCz). Multilayer devices fabricated using B2tCz or DB2tCz as hosts for the phosphorescence emitter, iridium(III)bis[(4,6-di-fluorophenyl)pyridinato-*N*,*C*2′]picolinate (FIrpic), showed maximum current efficiencies of 43.3 and 35.6 cd $A^{-1}$, power efficiencies of 34.0 and 29.4 lm $W^{-1}$, and external quantum efficiencies of 24.6% and 20.0%, respectively.



## Introduction

During the past few years, much progress has been made in the field of phosphorescent organic light-emitting diodes (OLEDs) because of their potential applications in full-color flat-panel displays and lighting sources. According to quantum statistics, in OLEDs with fluorescent dopants as emitters (fluorescent OLEDs), the light emission is attributed to singlet exciton formation, which imposes an upper limit of 25% on the theoretical quantum efficiency. Baldo *et al.* reported that the efficiency of OLEDs can be improved by employing phosphorescent dopants.[1] Phosphorescent organic light-emitting diodes (PhOLEDs) can capitalize on both singlet and triplet excitons to realize a theoretical internal quantum efficiency of 100%. Thus, a number of red- and green-light-emitting materials have already been identified for use in PhOLEDs. PhOLEDs based on the aforementioned materials are characterized by high luminous efficiency, reasonable color purity, and long lifetimes. Although there has been extensive research on blue PhOLEDs, achieving high electroluminescence (EL) performance remains a challenge because high bandgap energy and high triplet energy are required for blue emitters.

In PhOLEDs, properties of the host material generally determine the device performance, such as external quantum efficiency, current efficiency, and lifetime. This is because the triplet energy levels of the host materials should be higher than those of the phosphorescent dopants, in order to avoid triplet energy backtransfer from the dopant to the host and to confine triplet excitons to the emission zone. Designing host materials with these features remains a challenge for materials researchers. One of the most widely used host materials in blue PhOLEDs is 1,3-bis(carbazol-9-yl)benzene (mCP), which has high triplet energy ($E_T = 2.90$ eV) and good hole-transporting properties.[2] Although efficient energy transfer occurs from mCP to the dopant in the emitting layer because of the wide triplet energy bandgap of mCP, the relatively low thermal and morphological stability ($T_g = 65$ °C) of mCP may restrict its application as a host in blue PhOLEDs. Silicon-based wide-triplet-bandgap materials have been extensively studied to realize highly efficient blue PhOLEDs; however, deep HOMO energy levels make it difficult to balance hole and electron fluxes in the emission zone.[3] Recently, numerous host materials consisting of both electron-rich and electron-deficient functional groups have been reported to remarkably improve the device efficiency. These bipolar host materials can control energy levels and the hole- and electron-transporting ability. Additionally, the emitting materials should have an amorphous morphology since decreased crystallinity improves the device performance. Several bipolar molecules containing pyridine,[4] triazole,[5] borane,[6] quinoxaline,[7] bathophenanthroline,[8] benzimidazole,[9,10] oxadiazole,[11,12] phosphine oxide,[13] and phosphine sulfide[14] have been reported. These molecules have been used as the host for phosphorescent emitters or in single-layer fluorescence OLEDs. Although amine-containing molecules have been widely studied, fused sulfur-containing aromatic systems have rarely been investigated. In a recent publication, Lin reported a new blue phosphorescent host containing an electron-transporting dibenzothiophene molecular skeleton connected to a hole-transporting carbazolyl moiety.[15] This host material was designed to show high thermal stability, good transporting properties, and high triplet energy. An OLED

[a]*Department of Chemistry, College of Natural Sciences, Seoul National University, Seoul 151-747, Korea. E-mail: jihong@snu.ac.kr; Tel: +82 2 880 6682*
[b]*LG Display R&D Center, 1007 Deogeun-ri, Wollong-myeon, Paju-si, Gyeonggi-do, 413-811, Korea*

† Electronic supplementary information (ESI) available: DSC and mass spectra data for compounds B2tCz and DB2tCz. See DOI: 10.1039/c2jm34165d

device with CzDBS as the host material exhibited an external quantum efficiency of 9.2% (21.5 cd $A^{-1}$) at a brightness of 1000 cd $m^{-2}$ when the FIrpic dopant (iridium(III)bis[(4,6-di-fluorophenyl)pyridinato-*N*,*C*2′]picolinate) was used.[15] Additionally, Jeong introduced a dibenzothiophene (DBT) derivative with a carbazole or diphenylphosphinoxide moiety. OLED devices fabricated using 2,8-di(9*H*-carbazol-9-yl)dibenzo[*b*,*d*]thiophene (DBT1), 9-(8-(diphenylphosphoryl)dibenzo[*b*,*d*]thiophen-2-yl)-9*H*-carbazole (DBT2), and 2,8-bis(diphenylphosphoryl)dibenzo[*b*,*d*]thiophene (DBT3) as hosts along with FCNIrpic as the dopant exhibited external quantum efficiencies of 11.5%, 17.9%, and 16.0%, respectively.[16] Photophysical studies of fused thiophene compounds including [1]benzothiophene and dibenzothiophene revealed that the emission properties, phosphorescence lifetimes and quantum yields strongly depended on the number of rings and thiophene orientation along the long axis of the (*syn*, *anti*) molecular structures.[17] These results prompted us to apply sulfur-containing aromatic systems, benzo[*b*]thiophene (BT) and DBT, which have high triplet energy levels ($E_T$ = 3.02 eV and 3.06 eV, respectively) and good electron-transporting properties, to the blue PhOLEDs.

Herein, we report the design, synthesis, and characterization of new bipolar phosphorescent host materials having BT or DBT substituents with electron-transporting properties and carbazole moieties with hole-transporting properties. Until now, only a few examples of hosts having a DBT moiety have been reported as mentioned above. However, hosts having a BT moiety have not been used for blue PhOLEDs. The performance of the PhOLEDs doped with FIrpic is investigated. The devices show improved performance with a current efficiency of 40.8 cd $A^{-1}$, a power efficiency of 29.51 lm $W^{-1}$, an external quantum efficiency of 23.2%, and CIE coordinates of (0.13, 0.32) at 100 cd $m^{-2}$ for 9′-(9-(benzothiophen-3-yl)-9′*H*-[9,3′,6′,9″]tercarbazole) (B2tCz) and a current efficiency of 34.4 cd $A^{-1}$, a power efficiency of 24.6 lm $W^{-1}$, an external quantum efficiency of 19.4%, and CIE coordinates of (0.13, 0.31) at 100 cd $m^{-2}$ for 9′-(9-(dibenzothiophen-2-yl)-9′*H*-[9,3′,6′,9″]tercarbazole) (DB2tCz). Both compounds show high EL performance and have potential applications in blue PhOLEDs and lighting sources.

## Results and discussion

### Synthesis

The synthesis routes to B2tCz and DB2tCz are shown in Scheme 1. CzG2on was synthesized according to literature methods.[18,19] The host materials were readily prepared through the reaction between CzG2on and 3-bromobenzothiophene (or 2-bromodibenzothiophene) in the presence of copper(I) iodide, potassium phosphate, and (±)-*trans*-1,2-diaminocyclohexane in 1,4-dioxane. The structures of the compounds were confirmed by $^1$H NMR spectroscopy, $^{13}$C NMR spectroscopy, and mass spectrometry (MS) (see ESI†).

### Thermal properties

The durability and lifetime of a device are correlated with the glass transition temperature ($T_g$).[20] The thermal behavior of B2tCz and DB2tCz was investigated by differential scanning calorimetry (DSC) and thermogravimetric analysis (TGA)

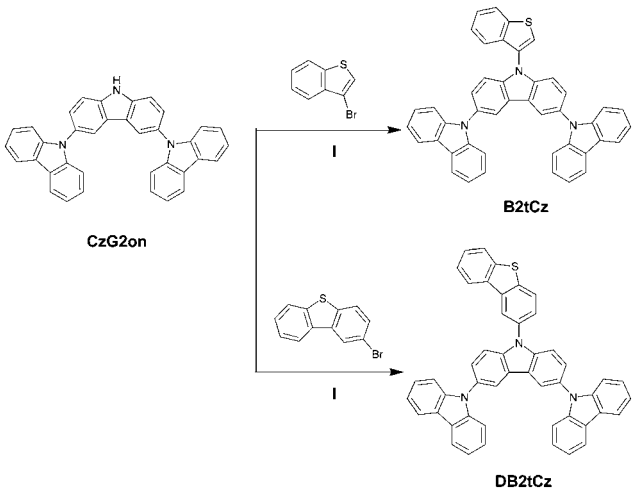


**Scheme 1** Synthesis of B2tCz and DB2tCz: (i) CuI, $K_3PO_4$, (±)-*trans*-1,2-diaminocyclohexane, 1,4-dioxane, 100 °C, 15 h.

(Fig. 1) under a nitrogen stream. DSC and TGA measurements were carried out from 25 to 400 °C and from 25 to 700 °C, respectively, at a scanning rate of 10 °C $min^{-1}$. The exact melting point of B2tCz was not found in our DSC experiments. However, the $T_g$ values for B2tCz and DB2tCz were measured to be 179 and 185 °C, respectively. Further, the decomposition temperatures ($T_d$) of these compounds were 492 and 515 °C, respectively. These temperatures were higher than those observed for mCP or other UGHs. The thermal stabilities of B2tCz and DB2tCz are also higher than those of previously reported materials. For example, CzDBS has a $T_g$ of 133 °C and a $T_d$ of 380 °C, respectively.[15] Furthermore, a 5% weight loss, observed at 403 and 439 °C, was attributed to the introduction of the carbazole unit. The high thermal stability of the host materials indicated that they are highly stable to endure the high temperatures at which vacuum vapor deposition is carried out.

### Cyclic voltammetry

The electrochemical properties of B2tCz and DB2tCz were investigated by cyclic voltammetry using anhydrous dichloromethane as the solvent, tetraethylammonium tetrafluoroborate

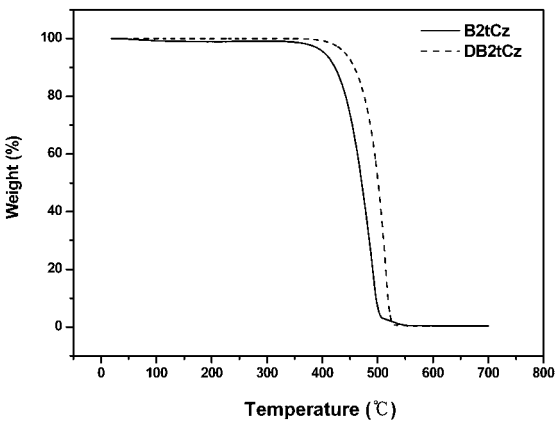


**Fig. 1** TGA of B2tCz and DB2tCz.

(0.1 M) as the supporting electrolyte, a platinum working electrode, and a Ag/AgCl reference electrode. On the basis of the highest occupied molecular orbital (HOMO) energy of the ferrocene/ferrocenium redox system (−4.8 eV), the HOMO energies of B2tCz and DB2tCz were calculated from the observed oxidation potentials to be −5.54 and −5.34 eV, respectively (Fig. 2).

## Optical properties

Fig. 3 shows the room-temperature UV-Vis absorption and photoluminescence (PL) spectra of B2tCz and DB2tCz in dichloromethane. The bandgap energies of B2tCz and DB2tCz were measured from the absorption edge of the UV-Vis absorption spectra. Calculated bandgaps from the data acquired for B2tCz and DB2tCz were 3.29 and 3.22 eV, respectively (Table 1). Thus, the lowest unoccupied molecular orbital (LUMO) energies were estimated to be −2.25 and −2.12 eV, respectively ($E_{LUMO}$ (eV) = $-(E_{HOMO} - E_g^{opt})$). These results revealed that the HOMO and LUMO energy levels of B2tCz and DB2tCz are almost similar. The low-temperature PL spectra of B2tCz and DB2tCz were obtained using a frozen solution (77 K) of 2-methyltetrahydrofuran (2-MeTHF). The low-temperature PL emission peaks of the new host materials were observed at approximately 437 ($E_T$ = 2.84 eV) and 423 nm ($E_T$ = 2.94 eV), respectively. These $T_1 \rightarrow S_0$ transition energies are higher than the estimated value for FIrpic ($E_T$ = 2.62 eV), *i.e.*, they are sufficiently high for B2tCz and DB2tCz to be used as host materials in blue PhOLEDs. The triplet states of DB2tCz are comparable to other phosphorescent blue host materials such as DBT2 ($E_T$ = 2.96 eV) with a phosphine oxide (PO) moiety.[16] As reported previously, the higher triplet energy of the host material would facilitate energy transfer from the host to the dopant in the host–guest system.[21] Accordingly, the two host materials synthesized in this study can be effective phosphorescent materials because energy backtransfer from the dopant to the host is prevented, and thus, the triplet excitons in the guest are effectively confined to the emission zone.

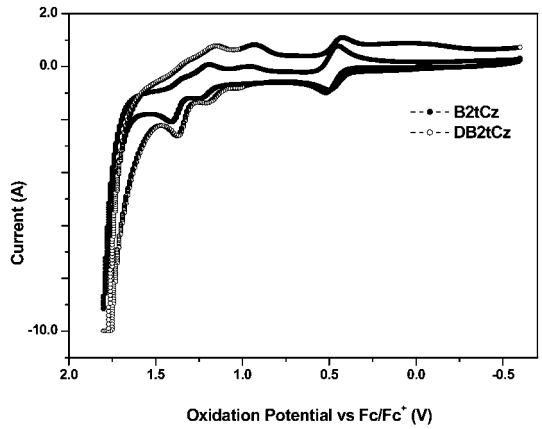


**Fig. 2** Cyclic voltammograms of B2tCz and DB2tCz.

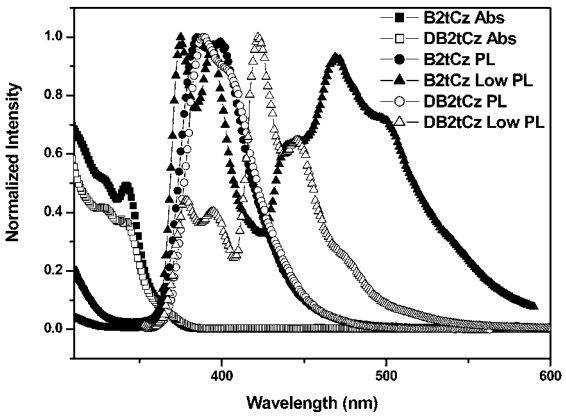


**Fig. 3** UV-Vis absorption and PL spectra of B2tCz and DB2tCz.

## Density functional theory calculations

To predict the optimized geometry and frontier molecular orbital levels for B2tCz and DB2tCz, density functional theory (DFT) calculations were carried out at the B3LYP/6-31G* level using Spartan '08.

As shown in Fig. 4, the calculated geometries of B2tCz and DB2tCz indicate that the carbazole moieties and thiophene substituents (benzothiophene or dibenzothiophene) are significantly twisted towards each other. These geometric properties can effectively hinder intermolecular interactions, which further implies that molecular recrystallization is prevented. The HOMOs of B2tCz and DB2tCz were delocalized over the

**Table 1** Thermal, electrochemical, and photophysical data for B2tCz and DB2tCz

| | B2tCz | DB2tCz |
|---|---|---|
| $T_g/T_m/T_d$ (°C) | 179/–/492 | 185/375/515 |
| $\lambda_{abs\ max}$ (nm)/$\lambda_{PL\ max}$ (nm) | 342/385 | 319/389 |
| HOMO/LUMO (eV) | −5.54/−2.25[a] | −5.34/−2.12[a] |
| | −5.19/−1.27[b] | −5.17/−1.43[b] |
| $E_T$ (eV) | 2.84 | 2.94 |

[a] From cyclic voltammetry. [b] From DFT calculations.

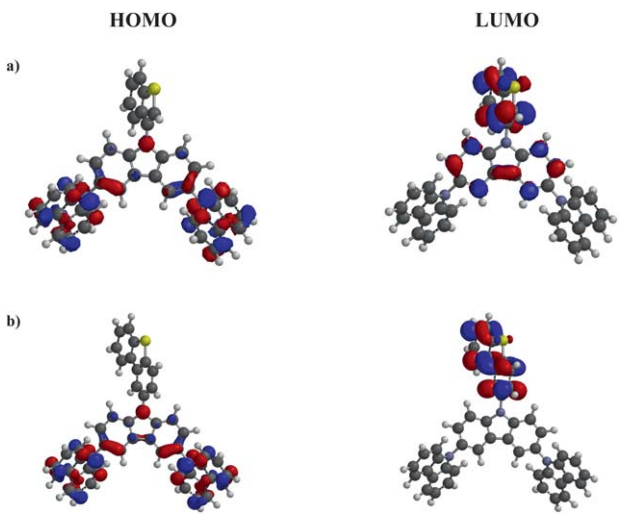


**Fig. 4** DFT calculations of (a) B2tCz and (b) DB2tCz.

 

carbazole moieties, indicating that each HOMO is mainly determined by the carbazole. In contrast, the LUMOs of B2tCz and DB2tCz showed a different behavior. The LUMO of B2tCz was delocalized between the central carbazole and benzothiophene; however, in the case of DB2tCz, significant separation was observed in the spatial distribution between the HOMO and the LUMO, because the HOMO is localized on the carbazole moiety (hole-transporting characteristics) and the LUMO resides at dibenzothiophene (electron-transporting characteristics).[10]

## Phosphorescent OLEDs

To compare the EL performances of the B2tCz and DB2tCz host materials for blue PhOLEDs with that of the mCP blue host, three sets of multilayer structures were fabricated: ITO/HATCN (50 Å)/NPB (550 Å)/TAPC (100 Å)/mCP: 10 wt% FIrpic (250 Å)/TmPyPB (300 Å)/LiF (5 Å)/Al (1000 Å) (device I), ITO/HATCN (50 Å)/NPB (550 Å)/TAPC (100 Å)/B2tCz: 10 wt% FIrpic (250 Å)/TmPyPB (300 Å)/LiF (5 Å)/Al (1000 Å) (device II), and ITO/HATCN (50 Å)/NPB (550 Å)/TAPC (100 Å)/DB2tCz: 10 wt% FIrpic (250 Å)/TmPyPB (300 Å)/LiF (5 Å)/Al (1000 Å) (device III). In each case, dipyrazino[2,3-*f*:2′,3′-*h*]quinoxaline-2,3,6,7,10,11-hexacarbonitrile (HATCN) was the hole-injection layer (HIL), *N*,*N*′-bis(naphthalene-1-yl)-*N*,*N*′-bis-(phenyl)benzidine (NPB) was the hole-transporting layer (HTL), di-[4-(*N*,*N*-ditolylamino)phenyl]cyclohexane (TAPC) was the electron-blocking layer (EBL) used to suppress the quenching of the FIrpic exciton at the HTL–EML interface, 1,3,5-tri[(3-pyridyl)phen-3-yl]benzene (TmPyPB) was the electron-transporting layer (ETL), and LiF was the electron-injection layer (EIL) at the LiF/Al cathode interface. The EL spectra of the three devices at 10 mA $cm^{-2}$ are shown in Fig. 5. The emission patterns of the three devices were almost similar to that of FIrpic, without any additional emission from the neighboring layers. These results indicated that complete energy transfer from the host to the dopant occurred and that the exciton was confined to the emission zone because the triplet level of the new host materials was higher than that of the dopant (FIrpic). Generally, FIrpic-based OLEDs show light-blue emission with CIE coordinates (*x*,*y*) of around (0.17, 0.34) because FIrpic shows the UV-Vis peak maximum at 472 nm and a vibrational peak at 500 nm.[22] The strong vibrational peak at 500 nm degraded the color performance of FIrpic doped device I, whereas the vibrational peak at 500 nm was slightly suppressed in device III, compared to that of device I. The difference in the color coordinates of devices I and III results from the different intensity of the shoulder peak of the FIrpic dopant. Moreover, devices I and III show different CIE color coordinates, because the emitting zone was shifted to the HTL side in the case of device III. Thus, device III exhibits more blue-shifted emissions with CIE coordinates (*x*,*y*) of (0.14, 0.31) at 100 cd $m^{-2}$ than that of device I with CIE coordinates (*x*,*y*) of (0.14, 0.33) at 100 cd $m^{-2}$ (Table 2). On the other hand, device II also exhibited a similar EL spectrum except for a larger shoulder peak at 500 nm compared to those of devices I and III. We guess that the larger shoulder peak at 500 nm in the case of device II comes from the longer wavelength tail of phosphorescence of B2tCz even extended to around 550 nm, which was longer than FIrpic emission.

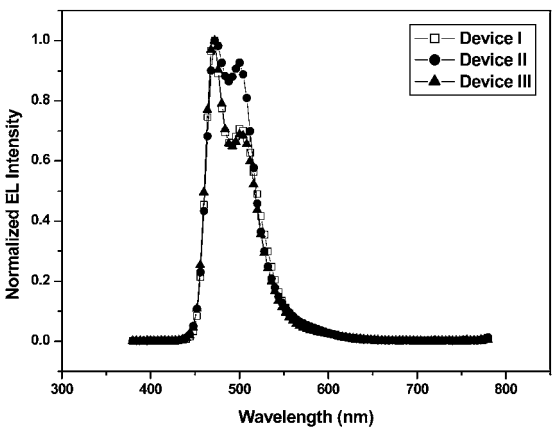


**Fig. 5** EL spectra of devices I, II, and III.

The EL performances of devices I, II, and III are shown in Fig. 6 and are summarized in Table 2. In particular, device I exhibited a maximum current efficiency ($\eta_c$) of 33.1 cd $A^{-1}$, a power efficiency ($\eta_p$) of 23.1 lm $W^{-1}$, and an external quantum efficiency ($\eta_{ext}$) of 18.1% at 5.2 V with CIE coordinates (*x*,*y*) of (0.14, 0.33). However, device II exhibited a maximum brightness of 6935 cd $m^{-2}$ at 9.8 V, with a maximum current efficiency ($\eta_c$) of 43.3 cd $A^{-1}$, a power efficiency ($\eta_p$) of 34 lm $W^{-1}$, and an external quantum efficiency ($\eta_{ext}$) of 24.6% at 4.0 V. Device III exhibited a maximum brightness of 4967 cd $m^{-2}$ at 10.4 V, a $\eta_c$ of 35.6 cd $A^{-1}$, $\eta_p$ of 29.4 lm $W^{-1}$, and $\eta_{ext}$ of 20.0% at 3.8 V. The devices fabricated using our blue phosphorescent host materials showed moderately low turn-on voltages of 3.6, 3.7, and 3.4 V at a luminance of 1 cd $m^{-2}$ as shown in Fig. 6. The difference in

**Table 2** EL performance of devices I and II with B2tCz and DB2tCz as blue phosphorescent hosts

| | Device I | | Device II | | Device III | |
|---|---|---|---|---|---|---|
| | At 100 cd $m^{-2}$ | ME | At 100 cd $m^{-2}$ | ME[f] | At 100 cd $m^{-2}$ | ME[f] |
| *V*[a] | 4.6 | 3.6 | 4.3 | 3.7[g] | 4.4 | 3.4[g] |
| CE[b] | 32.7 | 33.1 | 40.8 | 43.3 | 34.4 | 35.6 |
| PE[c] | 22.3 | 23.1 | 29.51 | 34.0 | 24.6 | 29.4 |
| EQE[d] | 17.9 | 18.1 | 23.2 | 24.6 | 19.4 | 20.0 |
| CIE[e] | (0.14, 0.33) | (0.14, 0.33) | (0.13, 0.32) | (0.13, 0.32) | (0.14, 0.31) | (0.14, 0.31) |

[a] Voltage. [b] Current efficiency. [c] Power efficiency. [d] External quantum efficiency. [e] CIE coordinates. [f] Maximum efficiency. [g] The applied voltage ($V_{on}$) required for a brightness of 1 cd $m^{-2}$.

turn-on voltages of devices I and II (or III) is due to the difference between the LUMO energy levels of host materials, mCP (2.40 eV) and B2tCz (2.25 eV) (or DB2tCz (2.12 eV)), and the electrode. These results indicated that the performance of our devices was better than that reported by Lin *et al.*[15] and Jeong and Lee.[16]

Device II showed slightly higher operational voltage than device III, because of the energy barrier between the HOMOs of the HTL and the EML; the HOMO levels of B2tCz and DB2tCz were 5.54 eV and 5.34 eV, respectively.

The lower operational voltage of device III could be attributed to the fact that the HOMO level of DB2tCz is almost similar to that of NPB for hole injection (Fig. 7).[23] Devices II and III exhibited $\eta_c$ of 40.8 and 34.4 cd $A^{-1}$, $\eta_p$ of 29.5 and 24.6 lm $W^{-1}$, $\eta_{ext}$ of 23.2 and 19.4%, and CIE coordinates of (0.13, 0.32) and (0.13, 0.31) at a brightness of 100 cd $m^{-2}$, respectively. The EL performance of the blue PhOLEDs was comparable to that mentioned in a previous report on the FIrpic dopant.[24] Additionally, quantum efficiency roll-off in devices II and III was observed upon increasing the brightness from 100 cd $m^{-2}$ to 1000 cd $m^{-2}$. Device II exhibited a $\eta_c$ of 35.0 cd $A^{-1}$, $\eta_p$ of 21.5 lm $W^{-1}$, $\eta_{ext}$ of 20.0%, and CIE coordinates of (0.13, 0.32) at a brightness of 1000 cd $m^{-2}$ while device III exhibited a $\eta_c$ of 27.4 cd $A^{-1}$, $\eta_p$ of 15.2 lm $W^{-1}$, and $\eta_{ext}$ of 15.5% with CIE coordinates of (0.13, 0.31). Furthermore, the quantum efficiency roll-off ratio of device II is lower than that of device III. We hypothesize that the lower roll-off ratio of device II is attributed to more balanced injection and transport of electrons and holes from the adjacent layers, ETL and HTL, in the emission zone.[25]

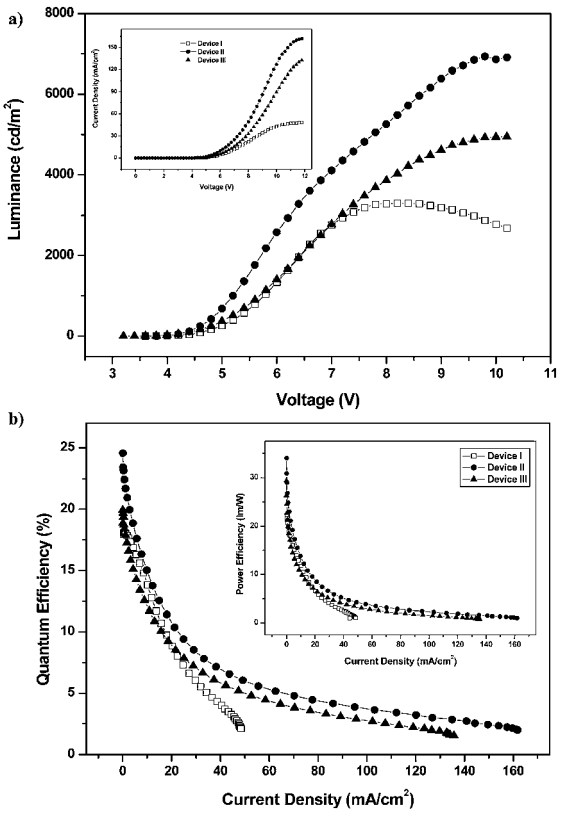


**Fig. 6** EL performance of devices I, II, and II. (a) Luminance and voltage characteristics of devices I, II and III. Inset: current density *vs.* voltage. (b) Quantum efficiency–current density characteristics of devices I, II, and III. Inset: power efficiency *vs.* current density.

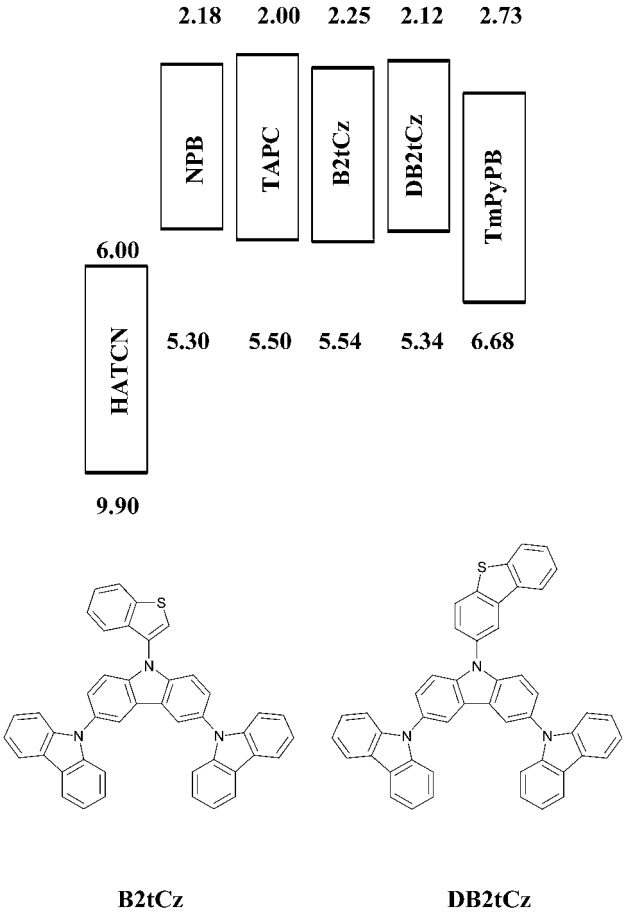


**Fig. 7** Energy diagram and chemical structures of materials used for fabrication of devices II and III.

## Conclusions

Two carbazole derivatives with sulfur-containing ring compounds, BT and DBT, were synthesized according to the literature procedure. The devices exhibited good thermal stability; the glass transition temperatures of B2tCz and DB2tCz were 179 and 185 °C, respectively. The decomposition temperatures of these compounds were 492 and 515 °C, respectively. In addition, the host materials showed good EL efficiency. B2tCz gave a current efficiency of 40.8 cd $A^{-1}$, a power efficiency of 29.4 lm $W^{-1}$, and an external quantum efficiency of 23.2% at a corresponding brightness of 100 cd $m^{-2}$ with CIE coordinates of (0.13, 0.32). DB2tCz gave a current efficiency of 34.4 cd $A^{-1}$, a power efficiency of 24.6 lm $W^{-1}$, and an external quantum efficiency of 19.4% at a corresponding brightness of 100 cd $m^{-2}$, with CIE coordinates of (0.13, 0.31). Additionally, both devices exhibited maximum current efficiencies of 43.3 and 35.6 cd $A^{-1}$, power efficiencies of 34.0 and 29.4 lm $W^{-1}$, and external quantum efficiencies of 24.6% and 20.0%, respectively. This level of performance is comparable to the highest values for previously reported sulfur-containing blue phosphorescent compounds.

 

## Experimental

### General information

All reagents and solvents were purchased from commercial sources and used without further purification, unless otherwise noted. $^1$H and $^{13}$C NMR spectra were recorded in $CDCl_3$ with $Me_4Si$ as the internal standard; all spectra were recorded using a Bruker 500 MHz spectrometer. Mass spectra were acquired using a Thermo Finnigan LTQ FT spectrometer with methanol as the carrier solvent. UV-Vis spectra were recorded using a SCINCO UVS 2100 spectrophotometer, and the optical bandgap was determined from the absorption onset of these spectra. TGA was performed with a Pyris 1 Thermal Gravimetric Analyzer (Perkin–Elmer), and DSC measurements were performed using a Mettler Toledo DSC 823 system. Cyclic voltammetry was performed with a 0.5 mM solution of the compounds, using an EG & G Princeton Applied Research Potentiostat & Galvanostat (Model 273A). Column chromatography was performed using Merck silica gel (70–230 mesh).

### Materials

**9′-(9-(Benzothiophen-3-yl)-9′*H*-[9,3′,6′,9]tercarbazole) (B2tCz).** *N*-Unsubstituted carbazole (CzG2on) (3.00 g, 6.03 mmol), 3-bromobenzothiophene (1.41 g, 6.63 mmol), copper iodide (0.12 g, 0.60 mmol), potassium phosphate (1.28 g, 6.03 mmol), (±)-*trans*-1,2-diaminocyclohexane (0.07 g, 0.60 mmol), and 1,4-dioxane (120 mL) were added to a 250 mL round-bottom flask equipped with a condenser and mechanical stirrer. The reaction mixture was heated to 100 °C for 15 h. After completion of the reaction, 50 mL of water was poured into the mixture to quench the reaction, and the resulting product was extracted with dichloromethane, purified by silica gel column chromatography (10% dichloromethane in *n*-hexane used as the eluent), and further purified by recrystallization. Yield: 82% (3.11 g, 4.94 mmol).

$^1$H NMR (500 MHz, $CDCl_3$): $\delta$ 8.29 (s, 2H), 8.15 (d, 4H, $J$ = 8.0 Hz), 8.04 (d, 1H, $J$ = 8.0 Hz), 7.84 (s, 1H), 7.58–7.37 (m, 15H), 7.29–7.23 (m, 4H); $^{13}$C NMR (125 MHz, $CDCl_3$): $\delta$ 141.80, 141.15, 139.24, 134.94, 130.66, 129.77, 126.67, 126.36, 125.90, 125.70, 125.02, 124.27, 124.02, 123.53, 123.23, 121.94, 120.30, 119.74, 111.94, 111.76, 109.71. HRMS (FT-MS) *m*/*z*: calcd for $[C_{44}H_{27}N_3S + H]^+$: 630.1926, found $[M + H]^+$: 630.1996. Anal. calcd for $C_{44}H_{27}N_3S$: C, 83.91; H, 4.32; N, 6.67; S, 5.09. Found: C, 83.56; H, 4.33; N, 6.64; S, 5.09%.

**9′-(9-(Dibenzothiophen-2-yl)-9′*H*-[9,3′,6′,9″]tercarbazole) (DB2tCz).** DB2tCz was synthesized according to the same procedure employed for B2tCz, except that 2-bromodibenzothiophene was used instead of 3-bromobenzothiophene. Yield: 86% (3.53 g, 5.19 mmol).$^1$H NMR (500 MHz, $CDCl_3$): $\delta$ 8.49 (s, 1H), 8.31 (s, 2H), 8.24 (d, 1H, $J$ = 7.0 Hz), 8.17 (t, 5H, $J$ = 8.0 Hz), 7.96 (d, 1H, $J$ = 7.5 Hz), 7.80 (dd, 1H, $J$ = 8.3 Hz), 7.68–7.25 (m, 18H); $^{13}$C NMR (125 MHz, $CDCl_3$): $\delta$ 141.84, 141.19, 140.44, 139.37, 137.38, 134.94, 133.92, 130.53, 127.64, 126.41, 125.91, 125.82, 124.87, 124.51, 124.00, 123.22, 123.14, 121.99, 120.49, 120.31, 119.84, 119.73, 111.28, 109.71. HRMS (FT-MS) *m*/*z*: calcd for $[C_{48}H_{29}N_3S + H]^+$: 680.2082, found $[M + H]^+$: 680.2150. Anal. calcd for $C_{48}H_{29}N_3S$: C, 84.80; H, 4.30; N, 6.18; S, 4.72. Found: C, 84.42; H, 4.39; N, 6.19; S, 4.63%.

### Device fabrication and measurements

Dipyrazino[2,3-*f*:2′,3′-*h*]quinoxaline-2,3,6,7,10,11-hexacarbonitrile (HATCN), *N*,*N*′-bis(naphthalene-1-yl)-*N*,*N*′-bis(phenyl)benzidine (NPB), di-[4-(*N*,*N*-ditolylamino)phenyl]cyclohexane (TAPC), and 1,3,5-tri[(3-pyridyl)phen-3-yl]benzene (TmPyPB) were purchased from Luminescence Technology Corp. OLEDs were fabricated by vacuum deposition onto a patterned ITO glass that had been previously cleaned and treated with oxygen plasma. Blue PhOLEDs were sequentially fabricated onto the ITO substrates through thermal evaporation of organic layers (evaporation rate: 2 Å $s^{-1}$; base pressure: $3 \times 10^{-6}$ Torr). The EL spectra and CIE color coordinates were obtained using a Spectrascan PR650 photometer, and the current–voltage–luminescence (J–V–L) characteristics were measured using a Keithley 2400 source unit.

## Acknowledgements

This study was supported by the Basic Science Research Program through a NRF grant funded by the MEST of Korea for the Center for Next-Generation Dye-Sensitized Solar Cells (no. 2012-0000591). Additional funding was provided by the New and Renewable Energy Technology Development Program, KETEP grant (no. 20113020010070), funded by the Ministry of Knowledge Economy.

## References

1 M. A. Baldo, M. E. Thompson and S. R. Forrest, *Nature*, 2000, **403**, 750.
2 R. J. Holmes, S. R. Forrest, Y. J. Tung, R. C. Kwong, J. J. Brown, S. Garon and M. E. Thompson, *Appl. Phys. Lett.*, 2003, **82**, 2422.
3 X. Ren, J. Li, R. J. Holmes, P. I. Djurovich, S. R. Forrest and M. E. Thompson, *Chem. Mater.*, 2004, **16**, 4743.
4 S.-J. Su, C. Cai and J. Kido, *Chem. Mater.*, 2011, **23**, 274.
5 M. K. Kim, J. Kwon, T.-H. Kwon and J.-I. Hong, *New J. Chem.*, 2010, **34**, 1317.
6 J. Doi, M. Kimoshita, K. Okumoto and Y. Shirota, *Chem. Mater.*, 2003, **15**, 10804.
7 C.-T. Chen, Y. Wei, J.-S. Lin, M. V. R. K. Moturu, W.-S. Chao, Y.-T. Tao and C.-H. Chien, *J. Am. Chem. Soc.*, 2006, **128**, 10992.
8 Z. Ge, T. Hayakawa, S. Ando, M. Ueda, T. Akiike, H. Miyamoto, T. Kajita and M. Kakimoto, *Org. Lett.*, 2008, **10**, 421.
9 M.-Y. Lai, C.-H. Chen, W.-S. Huang, J. T. Lin, T.-H. Ke, L.-Y. Chen, M.-H. Tsai and C.-C. Wu, *Angew. Chem., Int. Ed.*, 2008, **47**, 581.
10 Z. Y. Ge, T. Hayakawa, S. Ando, M. Ueda, T. Akiike, H. Miyamoto, T. Kajita and M. A. Kakimoto, *Adv. Funct. Mater.*, 2008, **18**, 584.
11 K. T. Kamtekar, C. Wang, S. Bettington, A. S. Batsanov, I. F. Perepichka, M. R. Bryce, J. H. Ahn, M. Rabinal and M. C. Petty, *J. Mater. Chem.*, 2006, **16**, 3823.
12 Y. Tao, Q. Wang, L. Ao, C. Zhong, J. Qin, C. Yang and D. Ma, *J. Mater. Chem.*, 2010, **20**, 1759.
13 S. O. Jeon, S. E. Jang, H. S. Son and J. Y. Lee, *Adv. Mater.*, 2011, **23**, 1436.
14 S. O. Jeon, K. S. Yook, C. W. Joo and J. Y. Lee, *Adv. Mater.*, 2010, **22**, 1872.
15 J.-S. Lin, M.-T. Lee, M.-T. Chu and M.-R. Tseng, *SID 11 DIGEST*, 1787.
16 S. H. Jeong and J. Y. Lee, *J. Mater. Chem.*, 2011, **21**, 14604.
17 B. Wex, B. R. Kaafarani, E. O. Danilov and D. C. Neckers, *J. Phys. Chem. A*, 2006, **110**, 13754.
18 K. Albrecht and K. Yamamoto, *J. Am. Chem. Soc.*, 2009, **131**, 2244.

19 J.-K. Bin, N.-S. Cho and J.-I. Hong, *Adv. Mater.*, 2012, **24**, 2911.
20 S. A. Van Slyke, C. H. Chen and C. W. Tang, *Appl. Phys. Lett.*, 1996, **69**, 2160.
21 C. Adachi, R. C. Kwong, P. Djurovich, V. Adamovich, M. A. Baldo, M. E. Thompson and S. R. Forrest, *Appl. Phys. Lett.*, 2001, **79**, 2082.
22 M.-H. Tsai, H.-W. Lin, H.-C. Su, T.-H. Ke, C.-C. Wu, F.-C. Fang, Y.-L. Liao, K.-T. Wong and C.-L. Wu, *Adv. Mater.*, 2006, **18**, 1216.
23 J.-K. Bin and J.-I. Hong, *Org. Electron.*, 2011, **12**, 802.
24 R.-F. Chen, G.-H. Xie, Y. Zhao, S.-L. Zhang, J. Yin, S.-Y. Liu and W. Huang, *Org. Electron.*, 2011, **12**, 1619.
25 C. Adachi, M. A. Baldo and S. R. Forrest, *J. Appl. Phys.*, 2000, **87**, 8049.



 